# DEVELOPMENT OF A MOLECULAR-BASED INDEX FOR ASSESSING IRON STATUS IN BLOOM-FORMING PENNATE DIATOMS[1]

*Adrian Marchetti,*[2] *Carly M. Moreno, Natalie R. Cohen*

Department of Marine Sciences, University of North Carolina at Chapel Hill, CB 3300, Chapel Hill, North Carolina 27599, USA

*Irina Oleinikov*

Department of Biomedical Science, Florida Atlantic University, 777 Glades Road, BC-71, Boca Raton, Florida 33431, USA

*Kimberly deLong*

Department of Marine Sciences, University of North Carolina at Chapel Hill, CB 3300, Chapel Hill, North Carolina 27599, USA

*Benjamin S. Twining*

Bigelow Laboratory for Ocean Sciences, 60 Bigelow Dr., PO Box 380, East Boothbay, Maine 04544, USA

*E. Virginia Armbrust*

School of Oceanography, University of Washington, Benjamin Hall IRB, 616 NE Northlake Place, Seattle, Washington 98105, USA

*and Robert H. Lampe*

Department of Marine Sciences, University of North Carolina at Chapel Hill, CB 3300, Chapel Hill, North Carolina 27599, USA

**Iron availability limits primary productivity in large areas of the world's oceans. Ascertaining the iron status of phytoplankton is essential for understanding the factors regulating their growth and ecology. We developed an incubation-independent, molecular-based approach to assess the iron nutritional status of specific members of the diatom community, initially focusing on the ecologically important pennate diatom *Pseudo-nitzschia*. Through a comparative transcriptomic approach, we identified two genes that track the iron status of *Pseudo-nitzschia* with high fidelity. The first gene, ferritin (*FTN*), encodes for the highly specialized iron storage protein induced under iron-replete conditions. The second gene, *ISIP*2a, encodes an iron-concentrating protein induced under iron-limiting conditions. In the oceanic diatom *Pseudo-nitzschia granii* (Hasle) Hasle, transcript abundance of these genes directly relates to changes in iron availability, with increased *FTN* transcript abundance under iron-replete conditions and increased *ISIP*2a transcript abundance under iron-limiting conditions. The resulting *ISIP*2a:*FTN* transcript ratio reflects the iron status of cells, where a high ratio indicates iron limitation. Field samples collected from iron grow-out microcosm experiments conducted in low iron waters of the Gulf of Alaska and variable iron waters in the California upwelling zone verify the validity of our proposed *Pseudo-nitzschia* Iron Limitation Index, which can be used to ascertain in situ iron status and further developed for other ecologically important diatoms.**

***Key index words:*** **diatoms; gene expression; iron status; molecular indicator; *Pseudo-nitzschia***

***Abbreviations*: ACT, actin; CUZ, California upwelling zone; DFB, desferrioxamine B; FLDA, flavodoxin; FTN, ferritin; ISIP, iron-starved-induced protein; KEGG, Kyoto Encyclopedia of Genes and Genomes; MMETSP, Marine Microbial Eukaryote Transcript Project; Ps-n ILI, *Pseudo-nitzschia* Iron Limitation Index; qPCR, quantitative polymerase chain reaction; TMC, trace metal clean**

Iron is predicted to be the primary limiting nutrient to phytoplankton growth within ~30%–40% of our oceans (Moore et al. 2002, Moore and Braucher 2007). In many oceanic regions, phytoplankton growth rates are chronically iron limited due to a low supply to surface waters (Johnson et al. 1997). In coastal regions where iron concentrations are variable, there is often extensive spatial and temporal patchiness in phytoplankton biomass due to ephemeral inputs of iron either from enhanced upwelling, mixing with high iron coastal waters and/or atmospheric deposition (Bruland et al. 2001, Moore and Braucher 2008). Diatoms are

[1]Received 19 November 2016. Accepted 9 March 2017. First Published Online 10 April 2017. Published Online 10 May 2017, Wiley Online Library (wileyonlinelibrary.com).

[2]Author for correspondence: e-mail amarchetti@unc.edu.

Editorial Responsibility: K. Müller (Associate Editor)

particularly susceptible to iron limitation, and a mechanistic understanding of ways that diatoms cope with low iron availability and respond rapidly to iron enrichment has come from a combination of field studies as well as studies with model species under controlled laboratory conditions (see review in Marchetti and Maldonado 2016). Iron-limited diatoms have reduced chlorophyll contents, photosynthetic efficiencies, and rates of N assimilation, attributes that contribute to reduced growth rates but are not specific to iron limitation.

Currently, nutrient amendment bioassays are the primary method used to elucidate the physiological status of natural phytoplankton communities. However, this approach requires an a priori assumption of the environmental factors regulating phytoplankton growth at each sampled point in space and time following a period of incubation. Incubation experiments that test whether iron is a limiting factor are time consuming and are often plagued by bottle artifacts (Scarratt et al. 2006). Iron measurements are confounded by complex iron speciation and the diversity of compounds that bind iron present within seawater, potentially influencing its biological availability (Bruland et al. 2014). A significant advancement would be the development of incubation-independent methods that evaluate iron nutritional status of select ecologically dominant members of a mixed phytoplankton community.

When iron limited, phytoplankton cells may temporarily replace iron-requiring proteins with less efficient iron-free functional equivalents to minimize their iron demands, including the well-described alternation between the iron-containing photosynthetic electron transfer protein ferredoxin and the iron-free version flavodoxin (La Roche et al. 1995, McKay et al. 1997). Most cultured isolates of diatoms preferentially use ferredoxin when grown under iron-replete conditions (McKay et al. 1999, Pankowski and McMinn 2009, Lommer et al. 2010). Therefore, the ratio of expressed ferredoxin protein relative to the combined ferredoxin and flavodoxin protein concentrations (known as the Fd index) has been employed as a measure of iron stress in bulk phytoplankton communities where a low ratio infers iron limitation (La Roche et al. 1996, Erdner and Anderson 1999). In addition, the examination of flavodoxin transcript abundance to infer the in situ iron status of specific diatoms has also been proposed (Chappell et al. 2015).

Although widely implemented, there are reported inconsistencies between laboratory and field studies when using the Fd index to elucidate iron status. For example, during the large-scale iron-enrichment experiment, IronExII, only flavodoxin was detected following iron enrichment, with no evidence of ferredoxin in any of the samples (Erdner and Anderson 1999). During the SERIES iron-enrichment experiment in the NE Pacific Ocean, expression of flavodoxin protein increased following iron enrichment rather than decreased, once again yielding unanticipated results (Boyd et al. 2005). Similarly, gene expression of flavodoxin in diatom populations increased substantially following iron enrichment within a comparative metatranscriptomic experiment in the same region, with very few transcripts of diatom ferredoxin detected (Marchetti et al. 2012). Lastly, there have been reported cases that many dominant, ecologically important diatoms constitutively use flavodoxin, either not expressing or having lost the ferredoxin gene altogether (Pankowski and McMinn 2009). Some diatoms contain multiple copies of flavodoxin, where only certain isoforms are differentially expressed in relation to iron status, further complicating its utility as an indicator of iron status (Whitney et al. 2011). Taken together, these studies suggest constitutive expression of flavodoxin in some oceanic diatoms may be common with little or no dependence on ferredoxin after the addition of iron to chronically iron-limited diatom communities. If this is indeed the case, the use of the Fd index as a measure of iron stress can be misleading and should be implemented with caution.

We have developed an incubation-independent molecular-based approach to assess the iron status of specific members of the phytoplankton community through querying the expression patterns of two iron-responsive genes. Our initial efforts have focused on *Pseudo-nitzschia*, a cosmopolitan pennate diatom genus that often exhibits large responses to iron enrichment and may produce the neurotoxin domoic acid (Bates et al. 1998). We performed a combination of laboratory and field experiments conducted within natural waters exhibiting either chronically low or variable iron concentrations where *Pseudo-nitzschia* is often a dominant member of the diatom community to validate our proposed *Pseudo-nitzschia* Iron Limitation Index (*Ps-n* ILI). We provide experimental evidence that further supports for the expansion of this molecular approach to other ecologically important diatoms found within different low iron regions, such as the Southern Ocean diatom *Fragilariopsis kerguelensis*.

## MATERIALS AND METHODS

*Algal culture conditions.* *Pseudo-nitzschia granii* UWOSP36 was obtained from Ocean Station Papa (OSP; 50° N, 145° W) in the Northeast Pacific Ocean (18S GenBank accession number KJ866907) in 2008. Cells were grown and maintained in acid-washed 28 mL polycarbonate centrifuge tubes at 12°C in semicontinuous batch cultures (Brand et al. 1981). All cultures were grown in Aquil medium using trace metal clean (TMC) techniques (Price et al. 1989). Macronutrients were added to Aquil medium in final concentrations of 300 $\mu mol \cdot L^{-1}$ $NO_3$, 10 $\mu mol \cdot L^{-1}$ $PO_4$, and 200 $\mu mol \cdot L^{-1}$ $Si(OH)_4$ to achieve macronutrient-replete growth. For media preparation, 2 L aliquots of Aquil were placed into acid-cleaned, Milli-Q™ (18.2 $M\Omega \cdot cm^{-1}$) $H_2O$-rinsed polycarbonate bottles. Dispensed seawater was sterilized by microwaving, then cooled and supplemented with filter-sterilized (0.2 μm Acrodisc) ethylenediaminetetraacetic acid (EDTA)-trace

metals (without iron) and vitamins (cobalamin, thiamine, and biotin) according to Price et al. (1989). Trace metal concentrations were buffered using 100 μmol · $L^{-1}$ of EDTA. Premixed iron-EDTA (1:1) was added separately at various total $FeCl_3$ concentrations between 1.5 and 12.9 nmol · $L^{-1}$ or 1,370 nmol · $L^{-1}$ to achieve iron-stressed/iron-limited cells or iron-replete cells, respectively. Predicted dissolved inorganic iron (Fe) concentrations (from MINEQL v. 4.6; Environmental Research Software, Hallowell, ME, USA) ranged from 3 to 26 pmol · $L^{-1}$ for the low iron medium and $2.74 \times 10^3$ pmol · $L^{-1}$ for the high iron medium (Table S1 in the Supporting Information). Media were allowed to equilibrate overnight before use and were stored in a TMC room. For the iron gradient experiment, cultures were grown on rotator tables under a continuous, saturating photon flux density of 150 μmol photons · $m^{-2}$ · $s^{-1}$ using soft-white fluorescent lights. Cell division in each iron treatment was considered acclimated when growth rates of successive transfers did not vary by more than 10% (typically 4–5 transfers). Although sterile techniques were used for all culture work to minimize bacterial contamination, cultures were not considered axenic.

To examine the effects of varying light and macronutrients (either Si or N) on the *Pseudo-nitzschia* ILI (see further description below), iron-replete (1,370 nmol · $L^{-1}$ $FeCl_3$) or iron-limited (1.5 nmol · $L^{-1}$ $FeCl_3$) cultures were grown in 2 L modified polycarbonate bottles with Teflon tubing to permit TMC subsampling at light levels of 60 μmol photons · $m^{-2}$ · $s^{-1}$ (low light), 150 μmol photons · $m^{-2}$ · $s^{-1}$ (growth saturating light), or 400 μmol photons · $m^{-2}$ · $s^{-1}$ (high light) using soft-white fluorescent lights and adjusted macronutrient concentrations of either 50 μmol · $L^{-1}$ Si $(OH)_4$ (resulting in Si depletion at stationary phase) or 50 μmol · $L^{-1}$ $NO_3$ (resulting in N depletion at stationary phase). All other Aquil components were kept constant as previously described. For the stationary time points, cultures were permitted to enter stationary phase for 2 d as assessed by a plateauing of relative chlorophyll *a* fluorescence. To ensure cells were in stationary phase due to either Si or N depletion (depending on the treatment), a subsample was spiked with either Si or N and chlorophyll *a* fluorescence was measured after 24 h to determine the impact on cell growth.

*Fragilariopsis kerguelensis* (O'Meara) Hustedt C L26-C5 was obtained from the Atlantic Sector of the Southern Ocean (48° S, 16° W) in 2009 (18S GenBank accession number KJ866919). Cells were maintained under similar conditions as described for *P. granii* except cultures were grown at 4°C, light levels of 10 μmol photons · $m^{-2}$ · $s^{-1}$ (low light) and 90 μmol photons · $m^{-2}$ · $s^{-1}$ (saturating light), and iron-limited growth was achieved at total iron concentrations of 3.1 nmol · $L^{-1}$ $FeCl_3$.

*Growth characterization.* Specific growth rates were calculated from the linear regression of the natural log of in vivo chlorophyll *a* fluorescence (using a Turner designs model 10-AU fluorometer, in vivo chlorophyll optical kit) versus time during the exponential growth phase of acclimated cells after confirming a proportional relationship between fluorescence and cell concentration (Brand et al. 1981). The response of maximum photochemical yield of PSII ($F_v$:$F_m$) to variations in iron concentrations and light levels was measured from fluorescence-induction measurements performed on cells in mid-exponential phase using a Walz Phyto-PAM fluorometer (*P. granii*) or a Satlantic FIRe (*Fragilariopsis kerguelensis*). Before each measurement, a subsample (5 mL) of each culture was placed in the dark for 20 min. For *Pseudo-nitzschia granii*, the constant fluorescence of dark-acclimated phytoplankton ($F_o$) was measured using modulated light at a low intensity (5 μmol quanta · $m^{-2}$ · $s^{-1}$) to avoid the reduction in the PSII primary electron acceptors. The maximal fluorescence yield ($F_m$) was induced by a short (200 ms) saturating pulse of light (3,500 μmol quanta · $m^{-2}$ · $s^{-1}$) to trigger the reduction in all PSII plastoquinone pools. $F_v$:$F_m$ was calculated as described in Schreiber et al. (1986) after the subtraction of a 0.2 μm filtered Aquil seawater blank. For *F. kerguelensis*, $F_v$:$F_m$ were measured from fluorescence-induction measurements performed using a Satlantic FIRe (Kolber et al. 1998, Gorbunov and Falkowski 2005). The resulting $F_v$:$F_m$ was derived from the induction profile using a saturating pulse (20,000 μmol photons · $m^2$ · $s^{-1}$) for a duration of 100–200 μs. The average of at least 10 iterations was obtained. Statistical analyses of growth rates and photophysiological data were performed with SigmaPlot 12.5 (Systat Software Inc., San Jose, Ca, USA). To test for significant differences between treatments, analysis of variance (ANOVA) was performed with a significance level set to $P < 0.05$. ANOVA also tests for normality using Shapiro-Wilk and Equal Variance tests. Post hoc Tukey tests were performed to determine which treatments differed significantly.

*Comparative transcriptomics in* Pseudo-nitzschia granii. The *P. granii* transcriptomes used here were sequenced to be included as reference libraries for annotation of environmental sequences obtained from an iron-enrichment experiment conducted at OSP (Marchetti et al. 2012), however, differential expression analysis of *P. granii* genes was not previously examined. Comparative transcriptomics were used to examine the whole cell gene expression response of iron-limited *P. granii* cells to a resupply of iron. To obtain enough mRNA for the 454 pyrosequencing and SOLiD sequencing, mRNA from three 20 L culture experiments was pooled. Iron-limited cells were collected both immediately prior to and 24 h following an iron resupply (herein referred to as iron-resupplied cells; Fig. S1 in the Supporting Information). Cells were collected onto 3.0 μm polycarbonate filters, immediately frozen in liquid nitrogen and stored at −80°C. RNA was extracted from thawed filters using the ToTALLY RNA extraction kit (Ambion® Thermo-Fisher Scientific, Waltham, MA, USA) according to the manufacturer's protocols with the additional step that filter pieces were first vortexed in 7 mL of denaturation solution containing 0.5 mL of glass beads and the resulting lysate was centrifuged at 8,801 *g* and 4°C for 3 min. The RNA was then incubated with deoxyribonuclease (DNase) I at 37°C for 45 min and purified by DNase I inactivation reagent. RNA concentrations were measured using a Nanodrop spectrophotometer. Polyadenosine [poly(A)+] RNA (mRNA) was isolated with the MicroPoly(A) Purist Kit (Ambion® Thermo-Fisher Scientific, Waltham, MA, USA) according to the manufacturer's instructions.

A combination of high-throughput sequencing platforms was used for sequencing, resulting in a single 454 sequence library from iron-resupplied cells and SOLiD sequence libraries from both iron-limited and iron-resupplied cells. For 454 pyrosequencing 10 μg of iron-resupplied *P. granii* mRNA was reverse transcribed into ds cDNA and sequenced using protocols as described in Marchetti et al. (2012). For SOLiD sequencing, 2.1 μg (iron limited) and 1.4 μg (iron resupplied) of *P. granii* ds cDNA were fragmented to an average size of 125 bp using a Covaris S2 System sonicator. The cDNA was then end-repaired using Polishing Enzymes 1 and 2 (Applied Biosystems® Thermo-Fisher Scientific, Waltham, MA, USA) to create blunt ends according to the SOLiD protocol. P1 and P2 adaptors were ligated to the cDNA, and the cDNA was nick-translated. PCR amplification was performed using 5 cycles and 2 cycles for iron-resupplied and iron-limited *P. granii* cDNA, respectively. The amplified cDNA fragments were purified using the PureLink PCR Purification Kit Invitrogen® Thermo-Fisher Scientific, Waltham, MA, USA. Each sample was diluted to 60 pg · $\mu L^{-1}$. Two and four emulsion PCRs were performed for iron-resupplied and iron-limited *P. granii* cDNA, respectively. Forty-one million beads of each sample were loaded onto two spots of an eight spot

slide, and run on an Applied Biosystems SOLiD sequencer version 3 Plus.

Protocols for sequence processing and clean-up are provided in Marchetti et al. (2012). Potential function of 454 reads was assigned based on best homology (BLASTx, *e*-value $\leq 10^{-3}$) to proteins within the Kyoto Encyclopedia of Genes and Genomes (KEGG). SOLiD reads were aligned to the iron-resupplied *P. granii* 454 reads to generate count data. Differential expression analysis was performed using the EdgeR method as outlined in Marchetti et al. (2012). All *P. granii* 454 sequences are deposited at NCBI's Sequence Read Archive under study accession number SRP006906.

*Gene expression (laboratory cultures).* *Pseudo-nitzschia granii* gene fragments for ferritin (*FTN*), iron-starvation-induced protein 2a (*ISIP*2a), and actin (*ACT*) were obtained from the *P. granii* 454 reads based on KEGG annotations and direct sequence searches. Full-length sequences for each target gene were constructed through assembly of SOLiD sequences with Velvet using the 454 read fragments as scaffolds. Primers for reverse transcription quantitative polymerase chain reaction (qPCR) were developed using Primer3 and tested using PCR, gel electrophoresis, and PCR product sequencing (Table S2 in the Supporting Information). RNA was extracted from thawed samples collected under the different iron and light treatments previously described using the RNAqueous-4PCR extraction kit (Invitrogen) according to the manufacturer's protocols. The RNA was incubated with DNase I at 37°C for 45 min and purified by DNase I inactivation reagent. RNA concentrations were measured using a Nanodrop spectrophotometer and samples with concentrations <250 ng $\cdot$ $\mu L^{-1}$ were concentrated using the RNeasy MinElute Cleanup Kit (Qiagen, Hilden, Germany). Quantitative PCR runs using the RNA samples were used to determine DNA contamination levels, with samples containing >10 DNA copies $\cdot$ $\mu L^{-1}$ of RNA incubated with DNase I and purified additional times as needed. Two microgram of each RNA sample was reverse transcribed into cDNA using Superscript III First Strand Synthesis Systems for RT-qPCR (Invitrogen). cDNA aliquots were diluted with water to obtain 60 µL total for each sample prior to use in qPCR.

The number of transcript copies of each gene of interest was quantified by qPCR in triplicate 20 µL reactions composed of 2 µL DNA standard or cDNA unknown, 10 µL Kapa SyberFast Universal qPCR Kit (Kapa Biosystems, MA, USA), and 1.6 µL of both forward and reverse primers. qPCR was run on an Eppendorf Mastercycler ep realplex. A dilution series of standards was run at the same time as experimental unknowns. Gene standards for qPCR were created by PCR amplification at 94°C for 2 min, followed by 40 cycles of 30 s at 95°C, 30 s at the specific primer's annealing temperature, and 1 min at 72°C. Reactions consisted of 1 µL DNA, 1 µL Taq Buffer, 1 µL $MgCl_2$, 0.5 µL dNTP, 0.4 µL of forward and reverse primers, 0.075 µL Taq polymerase, and 4.625 µL UV-light-treated water. Amplified fragments were cloned and transformed into *Escherichia coli* using the TOPO TA Cloning Kit (Invitrogen). Colonies containing the cloned gene fragment were incubated at 37°C overnight in liquid Luria broth media, and plasmids were extracted using QIAprep Spin Miniprep Kit (Qiagen). Plasmids were linearized through incubation with *SpeI* at 37°C for 1 h and enzyme denaturation at 80°C for 20 min. Linearized plasmids were quantified on a Qubit using the Qubit RNA Assay Kit (Invitrogen) and the copy number per µL was calculated. Serial dilutions with UV-light-treated water were used to create a series of standards for each gene of interest ranging from $10^6$ to $10^1$ copies $\cdot$ $\mu L^{-1}$. *P. granii ISIP*2a and *FTN* transcript copy numbers were either normalized to *ACT* copy numbers or each other from the same cDNA sample.

Gene sequences and read counts for *FTN* and *ISIP*2a from *F. kerguelensis* were obtained from the transcriptomes sequenced through the Marine Microbial Eukaryote Transcript Project (MMETSP; Keeling et al. 2014). Accession numbers and contig identification numbers of all target genes in *P. granii* and *F. kerguelensis* used in this study are provided in Table S2.

*Field experiments.* Field experiments were conducted on three separate cruises—two along the Line P transect in June of 2013 and 2015 on board the CCGS JP Tully and another in the California Upwelling Zone (CUZ) in July of 2014 on board the R/V Melville. On both of the Line P cruises, iron grow-out experiments were conducted at OSP (50° N, 145° W), a well-characterized iron-limited region (Harrison 2002). Seawater was collected at OSP from the depth corresponding to 30% of incident irradiance (10 m in 2013 and 12 m in 2015) using a TMC sampling system which consisted of a Teflon® air bellows pump and polytetrafluoroethylene-lined Kevlar™ tubing (0.75 in diameter) attached to Kevlar™ line. The seawater was placed into 10 L flexible acid-cleaned polyethylene cubitainers within a TMC-positive pressure flowhood. Cleaning protocols for the cubitainers included soaking the inside walls in 1.2 mol $\cdot$ $L^{-1}$ hydrochloric acid (reagent grade) for 3 d followed by three rinses with Milli-Q™ $H_2O$, soaking in 1.2 mol $\cdot$ $L^{-1}$ hydrochloric acid (trace metal grade) for 1 week followed by three rinses with Milli-Q™ $H_2O$, and soaking in 0.1 mol $\cdot$ $L^{-1}$ acetic acid (trace metal grade). Prior to filling the cubitainers with seawater, the dilute acetic acid was removed, and the cubitainers were rinsed thoroughly three times with ambient, low iron seawater. For each treatment, triplicate cubitainers were either inoculated with 4 nmol $\cdot$ $L^{-1}$ $FeCl_3$ or left unamended to serve as controls. In 2015, a 200 nmol $\cdot$ $L^{-1}$ desferrioxamine B (DFB) treatment was also included. DFB is a strong fungal siderophore that binds tightly to ferric iron, making it mostly unavailable for biological uptake by eukaryotic phytoplankton (Wells 1999, Marchetti and Maldonado 2016). For sample collection from initial conditions, triplicate cubitainers were immediately filtered. All other cubitainers were placed in on-deck plexiglass incubators with flow-through seawater to maintain near-ambient surface temperatures and were covered with neutral density screening to reduce irradiance to ~30% of the incident. All incubations were initiated and terminated just prior to dawn. Following 96 h of incubation, the seawater was removed from the incubators and stored in the dark at 4°C until filtration. Subsamples, for dissolved nutrients, chlorophyll *a* and RNA were collected from each cubitainer and immediately frozen at −20°C (nutrients and chlorophyll *a*) or −80°C (RNA). Dissolved nutrients and chlorophyll *a* protocols are provided in Marchetti et al. (2012), with the modification that analysis of thawed nutrients was performed onshore following the cruises.

During the CUZ cruise, multiple iron grow-out incubations were performed at different locations in relation to varying iron environments, including regions of high iron, upwelled waters, as well as relatively low iron waters. Treatments included a 5 nmol $\cdot$ $L^{-1}$ $FeCl_3$ addition, a 200 nmol $\cdot$ $L^{-1}$ DFB addition, and an unamended control. For two of the experiments, seawater was collected from the near surface (2–5 m) using a TMC sampling system which consisted of a towed GeoFish sampler attached to Kevlar™ line, Teflon® tubing, and a Teflon® dual-diaphragm pump that pumped seawater directly into a positive pressure TMC "bubble." The seawater was placed into a 200 L acid-cleaned, high-density polyethylene drum for homogenization before being distributed into 10 L flexible acid-cleaned polyethylene cubitainers cleaned using the same protocols as described previously and placed in on-deck plexiglass incubators with flow-through seawater to maintain near-ambient surface temperatures and were covered with neutral density screening to reduce irradiance to ~30% of the incident. Similar to the Line P cruises, all incubations were initiated and terminated just prior to

dawn. Following the incubation times, seawater filtrations were performed as described previously. For one experiment, seawater was obtained from the depth corresponding to the 10°C isotherm (96 m) and incubated on-deck to simulate an upwelling event.

For RNA extractions, seawater samples were filtered onto a Millipore Isopore membrane filter (0.4 μm pore size, 142 mm) by way of peristaltic pump and tygon tubing, flash frozen in liquid nitrogen, and stored at −80°C. In the laboratory, filters were briefly thawed on ice and total RNA was extracted from individual thawed filters using the ToTALLY RNA Kit (Ambion® Thermo-Fisher Scientific, Waltham, MA, USA) as described above. RNA samples were submitted to the UNC High-Throughput Sequencing Facility for library preparation (Illumina TruSeq Stranded mRNA Library Preparation Kit, HiSeq v4 reagents, including poly-A selection of mRNA), and each experiment was sequenced on a single lane using an Illumina HighSeq 2000. For the Line P experiments, RNA from the triplicate cubitainers was pooled prior to sequencing. For the CUZ experiments, most triplicate samples were sequenced separately except for two cases where the triplicates were pooled due to low RNA yields (Ctrl-72 and Fe-72 in experiment 4e). Each sample contained ~23 million 125 bp paired-end reads.

*Gene expression (field samples).* Raw reads were trimmed to remove low-quality bases and Illumina adapters using Trimmomatic v. 0.32 (paired-end mode, minimum read length of 36, adaptive quality trim with a target read length of 40 and strictness of 0.9; Bolger et al. 2014). Trimmed paired reads were merged into single reads with BBMerge v8.0, and merged pairs along with nonoverlapping paired-end reads were assembled using ABySS v1.5.2 with a multi-kmer approach (Simpson et al. 2009). Assemblies were merged using Trans-ABySS v1.5.3 (Vancouver, Canada) to remove redundant contigs (Robinson and Oshlack 2010) and contigs less than 120 bp were removed from libraries. Read counts were obtained by mapping raw reads to contigs through an end-to-end alignment using Bowtie2 v2.2.6 (Baltimore, MD, USA) (Langmead and Salzberg 2012). Alignments were filtered by mapping with quality scores of 10 or higher as determined by SAMtools v1.2 (Li et al. 2009). Taxonomic annotations were assigned based on sequence homology via BLASTx v2.3.0 (Bethesda, MD, USA) with an initial *e*-value cut-off of $10^{-3}$ against a custom-made protein database, MarineRefII, which is comprised of marine microbial eukaryote genomes and transcriptomes (Laboratory of Mary Ann Moran, University of Georgia). Environmental contigs were assigned a taxonomic annotation based on the top hit to a reference sequence in the MarineRefII database. In this study, only contigs assigned to the diatom genus *Pseudo-nitzschia* with *e*-values $<10^{-20}$ were included in the analysis. For determination of *Pseudo-nitzschia ISIP2A/FTN* ratios, *FTN* and *ISIP*2a sequences were obtained from the *P. granii* transcriptome and queried against *Pseudo-nitzschia*-associated contigs using tBLASTx v2.3.0 with an *e*-value cut-off of $10^{-3}$ for *FTN* and $10^{-5}$ for *ISIP*2a. All read counts corresponding to contigs with gene hits below the *e*-value threshold were summed within each treatment. All environmental sequences are deposited at NCBI's Sequence Read Archive under accession numbers SRP074366 (2013 Line P cruise) and PRJNA320398 (2014 IronBru and 2015 Line P cruises).

## RESULTS AND DISCUSSION

Sequencing of the comparative *Pseudo-nitzschia granii* transcriptome under variable iron states has provided new insights into an oceanic diatom that is well adapted to growing under low iron conditions. These include possession of important proteins for coping with low and ephemeral iron supply such as proteorhodopsin and *FTN* (Marchetti et al. 2009, 2015). It has also provided an opportunity to identify potential gene candidates to be used in the development of a molecular indicator for the iron status of *Pseudo-nitzschia* within natural mixed assemblages.

We identified two iron-related genes that were differentially expressed as a function of iron status. The first gene, *FTN*, encodes for the highly specialized iron storage protein that was relatively recently identified in diatoms (Marchetti et al. 2009). *FTN* genes have been identified in many different phytoplankton functional groups, including cyanobacteria (Theil et al. 2006). A *FTN* gene homolog is present in almost all pennate diatoms with sequenced genomes or transcriptomes and roughly half of sequenced centric diatoms (Groussman et al. 2015). *FTN* was one of the most highly enriched genes in iron-resupplied *P. granii* cells relative to iron-limited cells (Fig. 1a). The second gene, *ISIP*2a, encodes for a protein recently characterized in marine phytoplankton that concentrates iron at the cell surface and is believed to facilitate its uptake (Morrissey et al. 2015). *ISIP*2a is ubiquitously present across many phytoplankton functional groups, although it appears to be only present in marine algae. *ISIP*2a is a gene with one of the greatest accumulation of transcripts in the *P. granii* transcriptome and is highly enriched in iron-limited cells relative to iron-replete cells (Fig. 1a). Patterns of gene expression for both genes obtained from comparative transcriptomic sequencing were found to be consistent with expression trends obtained through targeted gene qPCR measurements (Fig. 1b).

Acclimated *P. granii* cells were grown under a gradient of iron concentrations to provide better resolution of the *FTN* and *ISIP*2a relative expression changes as a function of iron status. At the lowest iron concentration (1.5 nmol $\cdot$ $L^{-1}$ $Fe_T$), *P. granii* growth rates were substantially reduced, resulting in a 53% reduction relative to the maximum growth rate ($\mu_{max}$) achieved under iron-replete conditions (Fig. 2a). Subsequently, growth rates increased linearly as a function of iron up to a total iron concentration of 12.9 nmol $\cdot$ $L^{-1}$. At this iron concentration, the mean growth rate was not statistically different from $\mu_{max}$ ($F_{4,14}$ = 3.11, $P$ = 0.53), however, $F_v$:$F_m$ was significantly lower ($F_{4,14}$ = 3.11, $P$ = 0.038) than the maximum value of 0.66 achieved at the highest iron concentration, indicating iron stress (i.e., cells exhibit a physiological response to low iron conditions yet are able to maintain $\mu_{max}$; Fig. 2a). A further appreciable increase in the iron concentration yielded a minor enhancement in growth rate to $\mu_{max}$, indicating iron saturation was achieved at the highest iron concentrations examined. Relative gene expression of *P. granii FTN* was low at reduced iron concentrations and increased at high iron concentrations where growth rates were highest (Fig. 2b).

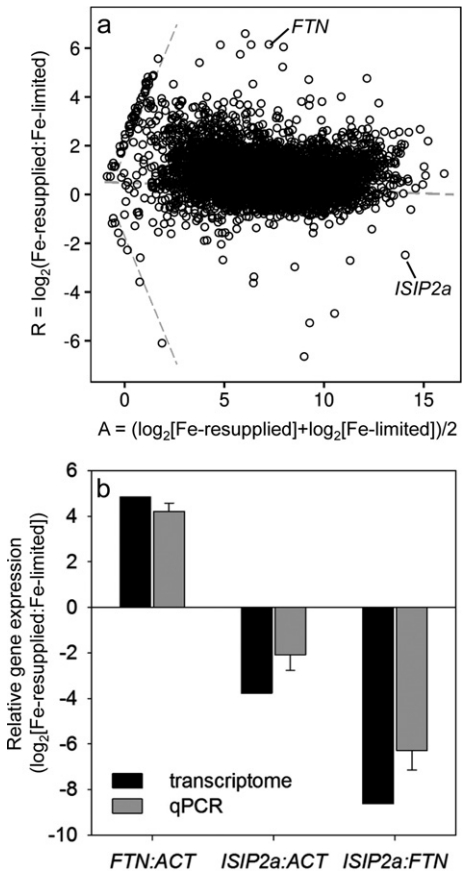


FIG. 1. Comparative transcriptome and gene expression in *Pseudo-nitzschia granii* as a function of iron. (a) Ratio-Average (RA) plot of *P. granii* differential gene expression in response to an iron-resupply to iron-limited cells. Each circle represents a collection of transcripts assigned to a predicted gene based on homology (BLASTx, *e*-value $\leq 10^{-3}$) and annotated via KEGG. Plotted are the log (base 2) fold-change ratio (R) and the average (A) of read counts in the iron-resupplied and iron-limited sequence libraries for a given gene. Gray horizontal line indicates the trimmed mean of fold-change values (TMM). Genes above or below the TMM indicate over- or underrepresentation, respectively, after iron resupply. Genes unique to one library are added into the plot left of the gray dashed lines. The gene circles for ferritin (*FTN*) and iron-starved-induced protein 2a (*ISIP*2a) are indicated. (b) A comparison of relative gene expression between the transcriptome (see a) and those obtained using quantitative PCR for *FTN* and *ISIP*2a when normalized to actin (*ACT*) and each other. Where provided, error bars are the standard deviation of the mean of triplicate cultures.

There was a 20-fold increase in relative gene expression for *FTN* as a function of iron status. In contrast, *ISIP*2a expression was high at low iron concentrations and then declined at the highest iron concentration examined. There was a 6-fold decrease in relative gene expression for *ISIP*2a as a function of iron status. The resulting *ISIP*2a:*FTN* ratio was highest under the most severe iron-limiting conditions. There was an 84-fold change in the *ISIP*2a:*FTN* ratio as a function of iron status: the maximum ratio of 1791 was obtained at the lowest growth rate and the minimum ratio of 21.2 was obtained at $\mu_{max}$ (Fig. 2c).

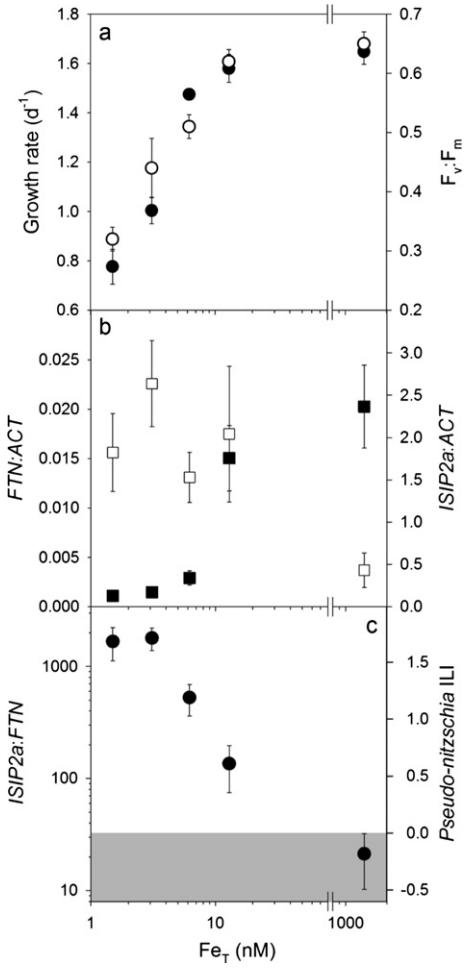


FIG. 2. Growth and gene expression characteristics in *Pseudo-nitzschia granii* as a function of iron concentration. (a) *P. granii* growth rates (closed circles) and maximum photochemical yields of PSII ($F_v$:$F_m$; open circles), (b) transcript copies of ferritin (*FTN*; closed squares) and iron-starved-induced protein 2a (*ISIP*2a; open squares) normalized to actin (*ACT*), and (c) expression of *ISIP*2a relative to *FTN* and the *Pseudo-nitzschia* Iron Limitation Index (*Ps-n* ILI; see methods) as a function of total iron concentrations in the presence of 100 $\mu mol \cdot L^{-1}$ EDTA (see Materials and Methods). Error bars are the standard deviation of the mean triplicate cultures.

The *Pseudo-nitzschia* ILI is a comparative measure of iron stress or limitation derived through the *ISIP*2a:*FTN* ratio. As determined from our laboratory growth experiments, the ratio for iron-replete *P. granii* cells was found to be $21.2 \pm 11.0$. Based on this threshold, we consider *Pseudo-nitzschia* growth as iron stressed or iron limited when the average *ISIP*2a:*FTN* ratio is found to be above 32.2 (mean + 1 SD). Using this criterion, we developed the *Ps-n* ILI as follows:

$$Ps\text{-}n\ \mathrm{ILI} = \log\left(\frac{ISIP2a}{1 + 32.2FTN}\right) \qquad (1)$$

where *ISIP*2a and *FTN* are the transcript abundances for each gene in a given sample's sequence library.

An additional advantage of our proposed two-gene expression ratio approach (where one gene response to iron limitation is opposite to the other) is that it amplifies the absolute range in values while providing for internal normalization across samples that is independent of sequencing depth. Accordingly, a positive value between 0 and 0.5 indicates iron-stressed cells, whereas values >0.5 indicates iron-limited growth. A negative value indicates iron-replete growth. Based on the *P. granii* culture experiments, the *Ps-n* ILI has a maximum upper limit of just below a value of two, which was achieved within the most severe iron-limited treatment in the culture experiments (Fig. 2c). However, in several of our examined field samples, *ISIP2*a transcripts were present without any *FTN* transcripts. In such instances a value for the *Ps-n* ILI would not be possible as this would result in an undefined fraction (denominator equal to 0), despite this ratio most likely indicating iron-limited growth. Therefore, a single transcript was added to the denominator in equation 1 to provide for a means to obtain a positive *Ps-n* ILI value (indicating iron limitation) under these instances. If *FTN* transcripts are absent in a given sample, we suggest that detection of more than 200 *ISIP*2a transcripts is necessary for the *Ps-n* ILI to indicate that *Pseudo-nitzschia* cells are iron limited. We have developed an online tool to calculate the *Ps-n* ILI from environmental mRNA libraries where *Pseudo-nitzschia* transcripts for *FTN* and *ISIP2a* are present (https://marchettilab.web.unc.edu/PsnILI/).

To examine whether additional environmental factors affect the *Ps-n* ILI, *P. granii* was grown under a combination of different irradiance levels where iron-replete and iron-limited cells entered stationary phase due to either a depletion of $NO_3$ or $Si(OH)_4$ from the growth medium. *Pseudo-nitzschia. granii* growth rates were primarily affected by iron status, with substantial reductions at all irradiance levels in the iron-limited treatments (Fig. 3, a, d and g; $F_{1,33} = 4.14$, $P < 0.001$). Both iron-replete and iron-limited growth rates were significantly reduced under low irradiance levels relative to the other irradiance treatments ($F_{2,33} = 3.29$, $P < 0.001$). There was an interactive effect between low light and iron where the combined treatment had the slowest growth rates compared to iron-limited cells grown at higher irradiance levels ($F_{2,33} = 3.29$, $P < 0.001$). At all irradiance levels, $F_v$:$F_m$ values were reduced due to iron limitation with only minor decreases with higher irradiance (Fig. 3, b, e and h). Further reductions in $F_v$:$F_m$ were observed in both iron-replete and iron-limited cells that entered stationary phase.

The *Ps-n* ILI values under all treatments were consistent with the iron gradient experiment where iron-limited, exponential phase *P. granii* cells exhibited a positive ILI and iron-replete exponential phase cells had a negative ILI (Fig. 3, c, f and i). When cells entered stationary phase due to either $NO_3$ or $Si(OH)_4$ depletion, in iron-limited diatoms the ILI remained positive. However, in several iron-replete treatments where cells entered stationary phase due to N depletion (e.g., low and high irradiances), the ILI also became slightly positive. This suggests that N depletion could also affect the expression patterns of *FTN* and/or *ISIP*2a, resulting in a positive *Ps-n* ILI. Thus, under conditions where N is suspected to be fully depleted, slightly positive ILI values (e.g., between 0 and 0.5) should be interpreted with caution.

We tested the validity of our proposed molecular indicator within natural phytoplankton communities within the Northeast Pacific Ocean known to harbor *Pseudo-nitzschia* populations. We calculated the *Ps-n* ILI within five separate iron grow-out experiments conducted within well-characterized iron-limited waters at OSP and within the iron limitation mosaic of the CUZ. In addition to unamended control, and iron-enriched treatments, 4 of the 5 experiments also included a treatment where DFB was added. Addition of DFB to seawater at higher concentrations than expected dissolved iron concentrations will reduce the biological availability of DFB-bound iron (Marchetti and Maldonado 2016). This treatment was used to induce iron stress and/or iron limitation in eukaryotic cells by preventing or substantially reducing the uptake of iron.

Ocean Station Papa (OSP) is one of the longest open ocean time series in the world, located in the NE subarctic Pacific Ocean in one of the three major iron-limited, high-nutrient, low-chlorophyll regions. Small cells dominate the phytoplankton community at OSP where large cells, such as diatoms, are chronically limited by low iron availability throughout the year in combination with limiting light levels during the winter months (Harrison 2002). In June of 2013 and 2015, the *Ps-n* ILIs of the initial seawater samples collected from within the mixed layer at OSP were positive (Fig. 4, a and b). Upon incubation for 96 h, *Ps-n* ILI values in the iron-enriched samples became negative, whereas the unamended controls in both years and a DFB addition treatment performed in the 2015 experiment remained positive (>1). The results of these experiments indicate that the ambient *Pseudo-nitzschia* populations present at OSP during both experimental periods were experiencing iron limitation that was alleviated by the addition of iron.

The CUZ is characterized by steep gradients in iron inputs over relatively short spatial scales that create neighboring areas of iron-replete and iron-limiting conditions (Bruland et al. 2001, Firme et al. 2003). These regions are differentiated primarily by the width of the continental shelf, which provides the primary source of iron through resuspension of sediment and associated reduced Fe(II) from the benthic boundary layer (Johnson et al. 1999, Chase et al. 2007). Dissolved iron concentrations can vary

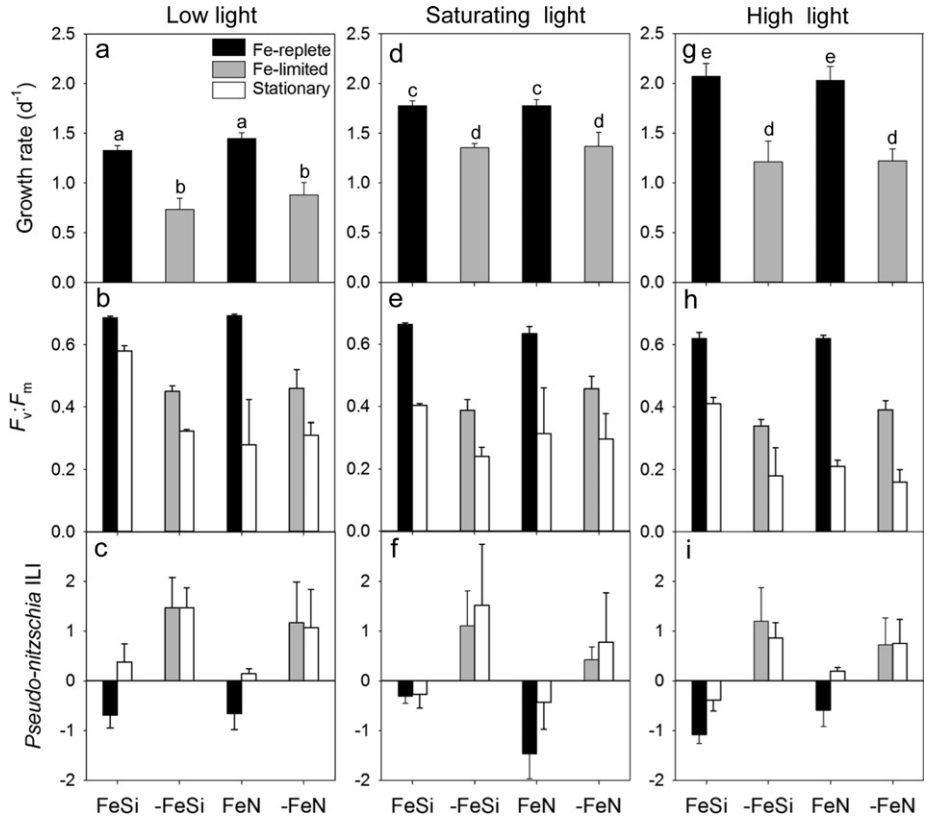


FIG. 3. Growth and gene expression characteristics in iron-replete and iron-limited *Pseudo-nitzschia granii* grown under varying light levels and macronutrient starvation conditions. *P. granii* (a, d, and g) growth rates, (b, e, and h) maximum photochemical yields of PSII ($F_v$:$F_m$) and (c, f, and i) *Pseudo-nitzschia* Iron Limitation Index (*Ps-n* ILI; see methods) of iron-replete, Si-starved at stationary phase (FeSi) cells; iron-limited, Si-starved at stationary phase (-FeSi) cells; iron-replete, N-starved at stationary phase (FeN) cells and iron-limited, N-starved at stationary phase (-FeN) cells grown under low-light (40 μmol quanta · $m^{-2}$ · $s^{-1}$; a–c), saturating light (150 μmol quanta · $m^{-2}$ · $s^{-1}$; d–f), or high-light (400 μmol quanta · $m^{-2}$ · $s^{-1}$; g–i) conditions. Error bars are the standard deviation of the mean triplicate cultures. In a, d, and g, letters above bars distinguish statistical differences among treatments (for iron treatments, $F_{1,33} = 4.14$, $P < 0.001$, and for light treatments, $F_{2,33} = 3.29$, $P < 0.001$).

100-fold from <0.1 nM in offshore waters to 10 nM in upwelling zones over the shelf (Biller and Bruland 2013, Biller et al. 2013). Concentrations of leachable/labile particulate matter are equally dynamic, ranging from 5 nM to over 200 nM in these upwelling and shelf gradients (Lohan and Bruland 2008, Biller et al. 2013). Labile particulate material such as freshly precipitated iron (oxy)hydroxides can be solubilized by dissolved organic ligands (Kraemer et al. 2005) and can serve as an important source of iron for phytoplankton (Hurst et al. 2010). In July of 2014, iron-enrichment experiments were performed throughout the CUZ as well as within upwelled waters off the coast of Oregon to assess the extent of iron limitation associated with recently upwelled waters from regions with both narrow and broad wide shelves. Due to the lack of upwelling present off the coast of Big Sur during the cruise period (Fig. 4e), waters were collected at a depth corresponding to the 10°C isotherm and incubated on the deck to simulate an upwelling event.

The initial *Ps-n* ILI values in two of three experiments within the CUZ were negative (Fig. 4, c and d). At the southern two sites, the *Ps-n* ILI remained negative in both control and iron-enriched treatments with only treatments where DFB was added becoming positive (Fig. 4, d and e). In contrast, at the site of natural upwelling off the coast of Oregon, the *Ps-n* ILI remained negative in only the iron-enriched treatment after 48 h of incubation, whereas the unamended control and DFB treatments both became positive (Fig. 4c). After 72 h of incubation, all *Ps-n* ILI values were positive, including the iron-enriched sample. The results of these experiments indicate that at all three sites, the ambient *Pseudo-nitzschia* populations were not iron limited. At the site of natural upwelling associated with a broad shelf (Fig. 4d) as well as in the simulated upwelling experiment (Fig. 4e), ambient iron concentrations were high enough to support the increases in biomass observed throughout the incubation period without cells entering iron stress (Fig. S2 in the Supporting Information). Thus, iron

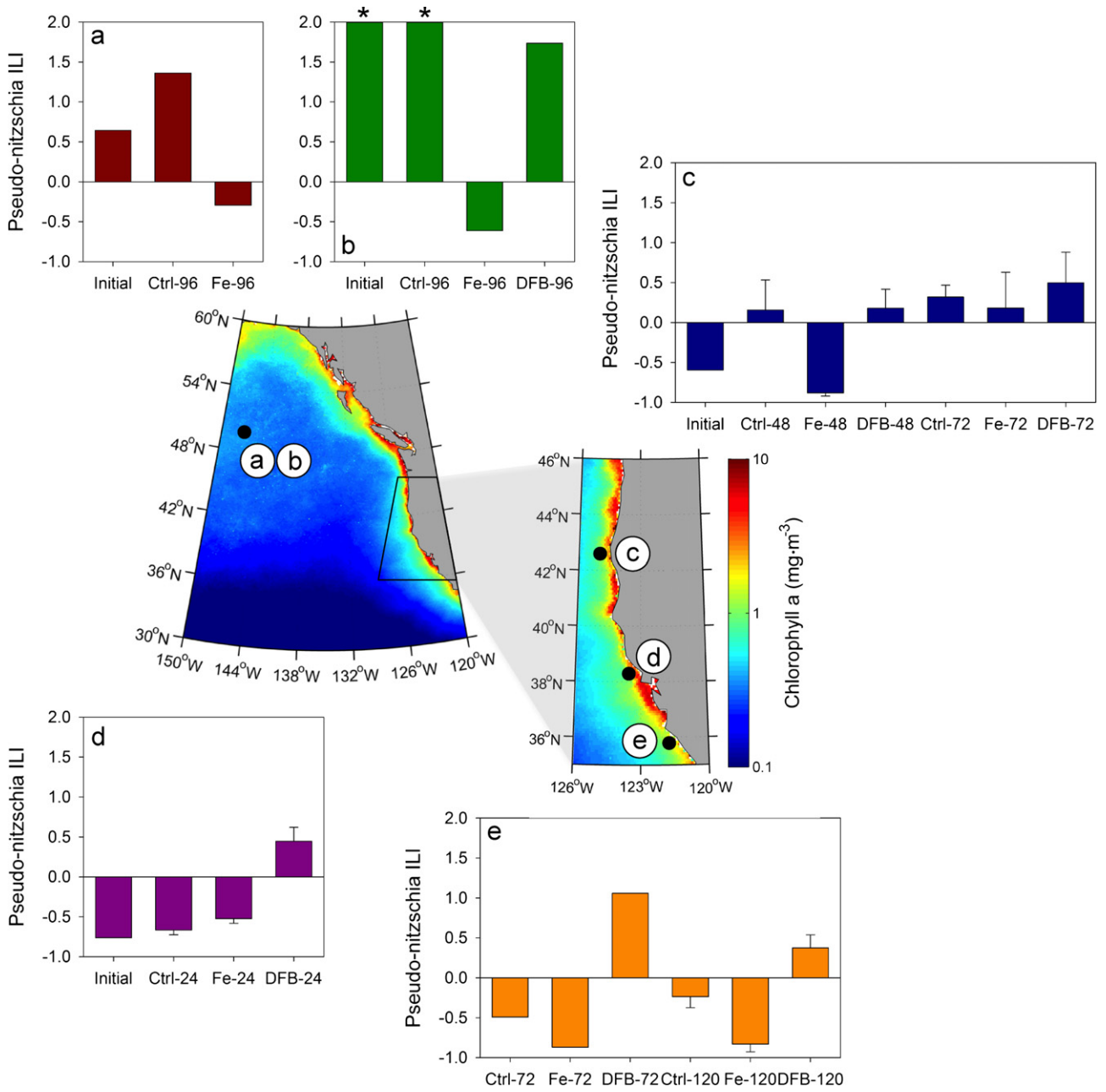


FIG. 4. *Pseudo-nitzschia* Iron Limitation Index (*Ps-n* ILI) values obtained from iron grow-out experiments with natural phytoplankton communities performed at Ocean Station Papa, Gulf of Alaska in (a) 2013 and (b) 2015, and the California Upwelling Zone (c–e) in 2014. Maps are climatological annual mean surface chlorophyll *a* concentrations from SeaWiFS (1997–2010) showing experiment sites. For each experiment, the initial *Ps-n* ILI is shown (except for e) in addition to values within an iron-amended treatment (Fe), unamended control treatment (Ctrl), and desferroxamine B treatment (DFB; except for a). Numbers denote incubation times in hours. In (e), initial *Ps-n* ILI was not obtained due to low transcript abundance. In (b), asterisks denote ILI values greater than 2 due to no detected *FTN* transcripts yet high abundances of *ISIP*2a transcripts. Where provided, error bars are the standard deviation of the mean of triplicate incubations. [Color figure can be viewed at wileyonlinelibrary.com]

stress/limitation of *Pseudo-nitzschia* cells in these waters was only induced upon addition of DFB. In contrast, in the naturally upwelled waters off the Oregon coast (Fig. 4c), despite the initial *Pseudo-nitzschia* populations not being iron limited, the increases in phytoplankton biomass within the first 48 h of incubation appear to have resulted in a reduction in bioavailable iron concentrations where the cells began to experience iron stress, albeit the *Ps-n* ILI in the unamended control treatments is only slightly positive. Unexpectedly, the *Ps-n* ILI in the iron-enriched treatment following 72 h of incubation was also positive, although it should be noted that at this time, $NO_3$ concentrations were very low

(<0.5 μmol · $L^{-1}$; Fig. S2), which may have affected the *Ps-n* ILI as observed in the laboratory cultures where *P. granii* cells that entered stationary phase due to N depletion also had slightly positive values.

Taken together, these incubation experiments verify the validity of the *Ps-n* ILI as an effective molecular indicator to ascertain the iron status of specific members of phytoplankton within natural, mixed assemblages. The *Ps-n* ILI provided expected values of *Pseudo-nitzschia* cells based on experiments within both oceanic and coastal waters. More importantly, our molecular approach highlights inherent weaknesses in evaluating the iron status of cells solely through nutrient amendment bioassays. Because incubation experiments typically require the observation of differential responses in biomass accumulation in iron-enriched treatments versus unamended controls over a period of time following incubation, it is difficult to assess what is an ambient stress in the preincubated samples versus one that has developed after some amount of biomass accumulation. An example of this is shown in Figure 4c (and Fig. S2), where based on the *Ps-n* ILI, the initial *Pseudo-nitzschia* cells were found not to be iron limited, although iron limitation quickly ensued after 48 h of incubation. A shift to positive ILI value in the control treatments likely occurred when the *Pseudo-nitzschia* cells became iron stressed as they divided and used up the available iron. These findings demonstrate the usefulness of differential gene expression approaches to rapidly and effectively evaluate in situ physiological status of select, ecologically dominant members of a mixed phytoplankton assemblage.

Chappell et al. (2015) recently proposed the use of expression patterns in the genes encoding flavodoxin (*FLDA1*) and an another iron-starvation-induced protein (*ISIP*3) as genetic indicators for iron status in the oceanic centric diatom *Thalassiosira oceanica* Hasle C. Transcript abundances for both genes increase in iron-limited *T. oceanica* relative to the housekeeping gene actin (Chappell et al. 2015). The general applicability of this indicator to other genera besides *Thalassiosira* is not yet clear. Consistent with their findings, transcript abundances for both *FLDA* and *ISIP*3 were significantly higher within iron-limited *P. granii* compared to iron-resupplied cells (Table S3 in the Supporting Information). However, during a comparative metatranscriptome study performed at OSP, transcripts associated with *P. granii FLDA* were found to be more abundant following iron enrichment (Marchetti et al. 2012). Interestingly, a gene encoding for ferredoxin within the *P. granii* transcriptome was not identified, suggesting this diatom, and perhaps others, do not use ferredoxin even under iron-replete conditions or may have lost the gene altogether and may thus depend on flavodoxin under all growth conditions. This raises uncertainties in using *FLDA* as an iron stress indicator for at least some diatoms, particularly those adapted to low iron environments. Similarly, within our *P. granii* comparative transcriptome, *ISIP*3 transcript abundance was relatively low compared to the other examined genes, even within iron-limited cells (Table S3) and expression appears to also be affected by light conditions (Chappell et al. 2015), which may be problematic in areas where both iron and light are known to be limiting to diatom growth (e.g., Southern Ocean).

Using the MMETSP database, Groussman et al. (2015) identified the presence of a putative *FTN* gene in 33 of 54 examined diatom species from 21 different genera, including both centric and pennate diatoms. Within several of these isolates, multiple *FTN* paralogs were identified, including in the diatom *Pseudo-nitzschia multiseries*. Similarly, it is feasible that the *FTN*s identified within and across algal lineages may perform multiple functional roles and therefore be expressed differently under the same environmental conditions. We therefore caution against the use of our proposed *Ps-n* ILI for other diatom species/genera without first testing to ensure resulting values obtained as a function of iron status are consistent with those in *P. granii*.

To examine whether our proposed *Ps-n* ILI could be used with other diatom genera, we grew *Fragilariopsis kerguelensis*, originally isolated from the polar Southern Ocean, under a range of iron and light conditions. *Fragilariopsis*, a genus of pennate diatoms closely related to *Pseudo-nitzschia* (Hasle 1965), are among the most dominant diatoms in polar plankton and sea ice (Garrison et al. 1987, Cefarelli et al. 2010). *Fragilariopsis* plays an important role within polar ecosystems as both the base of Antarctic food webs and as vectors for carbon and silicon transport from surface waters to deep ocean sediments. In fact, *F. kerguelensis* comprises 70% of the marine biogenic silicate sediments in the Southern Ocean (Treguer et al. 1995) and 80% of the diatom oozes (Zielinski and Gersonde 1997, Assmy et al. 2006). Consequently, *F. kerguelensis* not only represents a key species for the global silicate cycle but also indirectly controls the global carbon cycle via the storage of silicic acid. *Fragilariopsis* is highly responsive to iron enrichment, being the dominant diatom genus during the SOIREE (Gall et al. 2001) and EIFEX (Hoffmann et al. 2007) large-scale iron fertilization experiments, as well as being found in high abundances in naturally iron-fertilized waters (Blain et al. 2007, Timmermans et al. 2008). Members of this genus are also regarded as useful indicators of climate change (Melnikov et al. 2002).

*Fragilariopsis kerguelensis* growth rates and $F_v$:$F_m$ were reduced under low iron conditions (Fig. 5a). Similarly, low-light conditions reduced growth rates but had no apparent effects on photosynthetic efficiencies (Fig. 5b). In contrast to *P. granii*, there were no interactive effects of low iron and irradiance on *F. kerguelensis* growth rates, similar to what

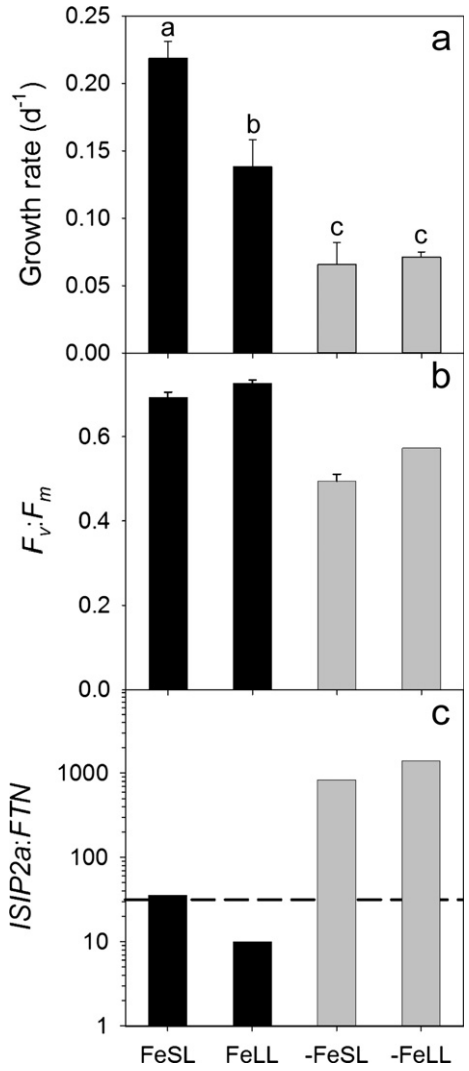


FIG. 5. Growth and gene expression characteristics in *Fragilariopsis kerguelensis* as a function of iron concentration and irradiance level. *F. kerguelensis* (a) growth rates, (b) maximum photochemical yields of PSII ($F_v$:$F_m$), and (c) expression of *ISIP*2a relative to *FTN* under iron-replete, saturating light (FeSL), iron-replete, low-light (FeLL), iron-limited, saturating light (-FeSL), and iron-limited, low-light (-FeLL) conditions. Black bars indicate iron-replete conditions and gray bars indicate iron-limited conditions. Dashed line in (c) indicates the *ISIP*2a:*FTN* threshold for *Pseudo-nitzschia* where a ratio greater than 32 suggests iron limitation. Where provided, error bars are the standard deviation of the mean of triplicate cultures. In (a), letters above bars distinguish statistical differences among treatments ($F_{1,11} = 4.84$, $P < 0.001$).

has been reported in other polar diatoms (Strzepek et al. 2012). Expression patterns of *ISIP*2a:*FTN* in *F. kerguelensis* are consistent with those of *Pseudo-nitzschia* when grown under variable iron and light conditions. In iron-replete cells, the resulting *ISIP*2a:*FTN* ratio remained below 32, whereas the iron-limited ratio was substantially higher, regardless of light status (Fig. 5c). These results support the development of an ILI with *Fragilariopsis*. Of particular importance is understanding the environmental controls on diatoms in the Southern Ocean, a region where both iron and light have been shown to limit growth of phytoplankton across short spatiotemporal scales (Boyd 2002, van Oijen et al. 2004) and where rapid changes in the environment due to global climate change are dramatically affecting plankton community dynamics and their associated influence on regional and global biogeochemistry (Constable et al. 2014). The implementation of our proposed *Fragilariopsis* ILI could be useful in providing this information.

This work was funded in part by NSF grants OCE0946260 to E.V.A. and A.M., OCE1334935 and PLR1341479 to A.M., and OCE1334632 to B.S.T. MMETSP was funded in part by the Gordon and Betty Moore Foundation through grant no. 2637 to the National Center for Genome Resources. We are grateful to R. Morales (UW) and D. Schruth for assistance with the *P. granii* transcriptome. We thank the scientists of the Line P program (IOS) and crew on the CCGS J.P. Tully as well as the scientists of the IrnBru 2014 cruise and the crew of the R/V Melville for assistance at sea with field experiments. Z. Li (Duke) assisted with climatological remote sensing images.

Assmy, P., Henjes, J., Smetacek, V. & Montresor, M. 2006. Auxospore formation by the silica-sinking, oceanic diatom *Fragilariopsis kerguelensis* (Bacillariophyceae). *J. Phycol.* 42:1002–6.

Bates, S. S., Garrison, D. L. & Horner, R. A. 1998. Bloom dynamics and physiology of domoic-acid-producing *Pseudo-nitzschia* species. *In* Anderson, D. M., Cembella, A. D. & Hallegraeff, G. M. [Eds] *Physiological Ecology of Harmful Algal Blooms.* Springer-Verlag, Heidelberg, pp. 267–92.

Biller, D. V. & Bruland, K. W. 2013. Sources and distributions of Mn, Fe Co, Ni, Cu, Zn, and Cd relative to macronutrients along the central California coast during the spring and summer upwelling season. *Mar. Chem.* 155:50–70.

Biller, D. V., Coale, T. H., Till, R. C., Smith, G. J. & Bruland, K. W. 2013. Coastal iron and nitrate distributions during the spring and summer upwelling season in the central California Current upwelling regime. *Cont. Shelf Res.* 66:58–72.

Blain, S., Queguiner, B., Armand, L., Belviso, S., Bombled, B., Bopp, L., Bowie, A. et al. 2007. Effect of natural iron fertilization on carbon sequestration in the Southern Ocean. *Nature* 446:1070–4.

Bolger, A. M., Lohse, M. & Usadel, B. 2014. Trimmomatic: a flexible trimmer for Illumina sequence data. *Bioinformatics* 30:2114–20.

Boyd, P. W. 2002. Environmental factors controlling phytoplankton processes in the Southern Ocean. *J. Phycol.* 38:844–61.

Boyd, P. W., Strzepek, R., Takeda, S., Jackson, G., Wong, C. S., McKay, R. M., Law, C. et al. 2005. The evolution and termination of an iron-induced mesoscale bloom in the northeast subarctic Pacific. *Limnol. Oceanogr.* 50:1872–86.

Brand, L. E., Sunda, W. & Guillard, R. R. L. 1981. A method for the rapid and precise determination of acclimated phytoplankton reproductive rates. *J. Plankton Res.* 3:193–201.

Bruland, K. W., Middag, R. & Lohan, M. C. 2014. Controls of trace metals in seawater. *In* Holland, H. D. & Tureklan, K. K. [Eds] *Treatise on Geochemistry*, 2nd edn, vol. 8. Elsevier, Oxford, pp. 19–51.

Bruland, K. W., Rue, E. L. & Smith, G. J. 2001. Iron and macronutrients in California coastal upwelling regimes: implications for diatom blooms. *Limnol. Oceanogr.* 46:1661–74.

Cefarelli, A. O., Ferrario, M. E., Almandoz, G. O., Atencio, A. G., Akselman, R. & Vernet, M. 2010. Diversity of the diatom genus *Fragilariopsis* in the Argentine Sea and Antarctic waters: morphology, distribution and abundance. *Polar Biol.* 33:1463–84.

Chappell, P. D., Whitney, L. P., Wallace, J. R., Darer, A. I., Jean-Charles, S. & Jenkins, B. D. 2015. Genetic indicators of iron limitation in wild populations of *Thalassiosira oceanica* from the northeast Pacific Ocean. *ISME J.* 9:592–602.

Chase, Z., Strutton, P. G. & Hales, B. 2007. Iron links river runoff and shelf width to phytoplankton biomass along the U.S. West Coast. *Geophys. Res. Lett.* 34:L04607.

Constable, A. J., Melbourne-Thomas, J., Corney, S. P., Arrigo, K. R., Barbraud, C., Barnes, D. K. A., Bindoff, N. L. et al. 2014. Climate change and Southern Ocean ecosystems I: how changes in physical habitats directly affect marine biota. *Global Change Biol.* 20:3004–25.

Erdner, D. L. & Anderson, D. M. 1999. Ferredoxin and flavodoxin as biochemical indicators of iron limitation during open-ocean iron enrichment. *Limnol. Oceanogr.* 44:1609–15.

Firme, G. F., Rue, E. L., Weeks, D. A., Bruland, K. W. & Hutchins, D. A. 2003. Spatial and temporal variability in phytoplankton iron limitation along the California coast and consequences for Si, N, and C biogeochemistry. *Global Biogeochem. Cycle* 17:1016.

Gall, M. P., Boyd, P. W., Hall, J., Safi, K. A. & Chang, H. 2001. Phytoplankton processes. Part 1: community structure during the Southern Ocean iron release experiment (SOIREE). *Deep Sea Res. Pt. II* 48:2551–70.

Garrison, D. L., Buck, K. R. & Fryxell, G. A. 1987. Algal assemblages in Antarctic pack ice and in ice-edge plankton. *J. Phycol.* 23:564–72.

Gorbunov, M. Y. & Falkowski, P. 2005. Fluorescence Induction and Relaxation (FIRe) technique and instrumentation for monitoring photosynthetic processes and primary production in aquatic ecosystems. *In* van der Est, A. & Bruce, D. [Eds.] *Proc. 13th International Congress of Photosynthesis.* Allen Press, Montreal, Quebec, pp. 1029–31.

Groussman, R. D., Parker, M. S. & Armbrust, E. V. 2015. Diversity and evolutionary history of iron metabolism genes in diatoms. *PLoS ONE* 10:e0129081.

Harrison, P. J. 2002. Station Papa time series: insights into ecosystem dynamics. *J. Oceanogr.* 58:259–64.

Hasle, G. R. 1965. *Nitzschia* and *Fragilariopsis* species studied in the light and electron microscopes II: the group *Pseudonitzschia*. *Skrifter utgitt av Det Norske Videnskaps-Akademi i Oslo I. Matematisk-Natuvidenskapelig Klasse. Ny Serie* 18:1–45.

Hoffmann, L. J., Peeken, I. & Lochte, K. 2007. Effects of iron on the elemental stoichiometry during EIFEX and in the diatoms *Fragilariopsis kerguelensis* and *Chaetoceros dichaeta*. *Biogeosciences* 4:569–79.

Hurst, M. P., Aguilar-Islas, A. M. & Bruland, K. W. 2010. Iron in the southeastern Bering Sea: elevated leachable particulate Fe in shelf bottom waters as an important source for surface waters. *Cont. Shelf Res.* 30:467–80.

Johnson, K., Chavez, F. & Friederich, G. 1999. Continental-shelf sediment as a primary source of iron for coastal phytoplankton. *Nature* 398:697–700.

Johnson, K. S., Gordon, R. M. & Coale, K. H. 1997. What controls dissolved iron concentrations in the world ocean? *Mar. Chem.* 57:137–61.

Keeling, P. J., Burki, F., Wilcox, H. M., Allam, B., Allen, E. E., Amaral-Zettler, L. A., Armbrust, E. V. et al. 2014. The Marine Microbial Eukaryote Transcriptome Sequencing Project (MMETSP): illuminating the functional diversity of eukaryotic life in the oceans through transcriptome sequencing. *PLoS Biol.* 12:e1001889.

Kolber, Z. S., Prasil, O. & Falkowski, P. G. 1998. Measurements of variable chlorophyll fluorescence using fast repetition rate techniques - defining methodology and experimental protocols. *Biochim. Biophys. Acta* 1367:88–106.

Kraemer, S. M., Butler, A., Borer, P. & Cervini-Silva, J. 2005. Siderophores and the dissolution of iron-bearing minerals in marine systems. *Rev. Mineral. Geochem.* 59:53–84.

La Roche, J., Boyd, P., McKay, R. & Geider, R. 1996. Flavodoxin as an in situ marker for iron stress in phytoplankton. *Nature* 382:802–5.

La Roche, J., Murray, H., Orellana, M. & Newton, J. 1995. Flavodoxin expression as an indicator of iron limitation in marine diatoms. *J. Phycol.* 31:520–30.

Langmead, B. & Salzberg, S. L. 2012. Fast gapped-read alignment with Bowtie 2. *Nat. Meth.* 9:357–9.

Li, H., Handsaker, B., Wysoker, A., Fennell, T., Ruan, J., Homer, N., Marth, G., Abecasis, G., Durbin, R. & Subgroup, G. P. D. P. 2009. The sequence alignment/map format and SAMtools. *Bioinformatics* 25:2078–9.

Lohan, M. C. & Bruland, K. W. 2008. Elevated Fe(II) and dissolved Fe in hypoxic shelf waters off Oregon and Washington: an enhanced source of iron to coastal upwelling regimes. *Environ. Sci. Technol.* 42:6462–8.

Lommer, M., Roy, A., Schilhabel, M., Schreiber, S., Rosenstiel, P. & LaRoche, J. 2010. Recent transfer of an iron-regulated gene from the plastid to the nuclear genome in an oceanic diatom adapted to chronic iron limitation. *BMC Genom.* 11:718.

Marchetti, A., Catlett, D., Hopkinson, B. M., Ellis, K. & Cassar, N. 2015. Marine diatom proteorhodopsins and their potential role in coping with low iron availability. *ISME J.* 9:2745–8.

Marchetti, A. & Maldonado, M. T. 2016. Iron. *In* Borowitzka, M. A., Beardall, J. & Raven, J. A. [Eds] *The Physiology of Microalgae.* Springer, Cham, Switzerland, pp. 233–79.

Marchetti, A., Parker, M. S., Moccia, L. P., Lin, E. O., Arrieta, A. L., Ribalet, F., Murphy, M. E. P., Maldonado, M. T. & Armbrust, E. V. 2009. Ferritin is used for iron storage in bloom-forming marine pennate diatoms. *Nature* 457:467–70.

Marchetti, A., Schruth, D. M., Durkin, C. A., Parker, M. S., Kodner, R. B., Berthiaume, C. T., Morales, R., Allen, A. E. & Armbrust, E. V. 2012. Comparative metatranscriptomics identifies molecular bases for the physiological responses of phytoplankton to varying iron availability. *Proc. Natl. Acad. Sci. USA* 109:E317–25.

McKay, R. M. L., Geider, R. J. & LaRoche, J. 1997. Physiological and biochemical response of the photosynthetic apparatus of two marine diatoms to Fe stress. *Plant Physiol.* 114:615–22.

McKay, R. M. L., La Roche, J., Yakunin, A. F., Durnford, D. G. & Geider, R. J. 1999. Accumulation of ferredoxin and flavodoxin in a marine diatom in response to iron. *J. Phycol.* 35:510–9.

Melnikov, I. A., Kolosova, E. G., Welch, H. E. & Zhitina, L. S. 2002. Sea ice biological communities and nutrient dynamics in the Canada Basin of the Arctic Ocean. *Deep Sea Res. Pt. I* 49:1623–49.

Moore, J. K. & Braucher, O. 2007. Observations of dissolved iron concentrations in the World Ocean: implications and constraints for ocean biogeochemical models. *Biogeosci. Disc.* 4:1241–77.

Moore, J. K. & Braucher, O. 2008. Sedimentary and mineral dust sources of dissolved iron to the world ocean. *Biogeosciences* 5:631–56.

Moore, J. K., Doney, S. C., Glover, D. M. & Fung, I. Y. 2002. Iron cycling and nutrient-limitation patterns in surface waters of the World Ocean. *Deep Sea Res. Pt. II* 49:463–507.

Morrissey, J., Sutak, R., Paz-Yepes, J., Tanaka, A., Moustafa, A., Veluchamy, A., Thomas, Y. et al. 2015. A novel protein, ubiquitous in marine phytoplankton, concentrates iron at the cell surface and facilitates uptake. *Curr. Biol.* 25:364–71.

van Oijen, T., Van Leeuwe, M. A. & Granum, E. 2004. Light rather than iron controls photosynthate production and allocation in Southern Ocean phytoplankton populations during austral autumn. *J. Plankton Res.* 26:885–900.

Pankowski, A. & McMinn, A. 2009. Iron availability regulates growth, photosynthesis, and production of ferredoxin and flavodoxin in Antarctic sea ice diatoms. *Aquatic Biology* 4:273–88.

Price, N. M., Harrison, G. I., Hering, J. G., Hudson, R. J., Nirel, P. M. V., Palenik, B. & Morel, F. M. M. 1989. Preparation and chemistry of the artificial algal culture medium Aquil. *Biological Oceanogr.* 6:443–61.

Robinson, M. & Oshlack, A. 2010. A scaling normalization method for differential expression analysis of RNA-seq data. *Genome Biol.* 11:R25.

Scarratt, M. G., Marchetti, A., Hale, M. S., Rivkin, R. B., Michaud, S., Matthews, P., Levasseur, M., Sherry, N. D., Merzouk, A., Li, W. K. W. & Kiyosawa, H. 2006. Assessing microbial responses to iron enrichment in the Subarctic Northeast Pacific: do microcosms reproduce the in situ condition?. *Deep Sea Res. Pt. II* 53:2182–200.

Schreiber, U., Schliwa, U. & Bilger, W. 1986. Continuous recording of photochemical and nonphotochemical chlorophyll fluorescence quenching with a new type of modulation fluorometer. *Photosynthesis Res.* 10:51–62.

Simpson, J. T., Wong, K., Jackman, S. D., Schein, J. E., Jones, S. J. M. & Birol, İ. 2009. ABySS: a parallel assembler for short read sequence data. *Genome Res.* 19:1117–23.

Sunda, W. G., Price, N. M. & Morel, F. M. M. 2005. Trace metal ion buffers and their use in culture studies. *In*: Andersen R. A. [Ed.] *Algal culturing techniques*. Elsevier Academic Press, San Diego, CA, USA, pp. 35–63.

Strzepek, R. F., Hunter, K. A., Frew, R. D., Harrison, P. J. & Boyd, P. W. 2012. Iron-light interactions in Southern Ocean phytoplankton. *Limnol. Oceanogr.* 57:1182–200.

Theil, E. C., Matzapetakis, M. & Liu, X. 2006. Ferritins: iron/oxygen biominerals in protein nanocages. *JBIC Journal of Biological Inorganic Chemistry* 11:803–10.

Timmermans, K. R., Veldhuis, M. J. W., Laan, P. & Brussaard, C. P. D. 2008. Probing natural iron fertilization near the Kerguelen (Southern Ocean) using natural phytoplankton assemblages and diatom cultures. *Deep Sea Res. Pt. II* 55:693–705.

Treguer, P., Nelson, D. M., Van Bennekom, A. J., DeMaster, D. J., Leynaert, A. & Queguiner, B. 1995. The silica balance in the world ocean: a reestimate. *Science* 268:375–9.

Wells, M. L. 1999. Manipulating iron availability in nearshore waters. *Limnol. Oceanogr.* 44:1002–8.

Whitney, L. P., Lins, J. J., Hughes, M. P., Wells, M. L., Chappell, P. D. & Jenkins, B. D. 2011. Characterization of putative iron responsive genes as species-specific indicators of iron stress in thalassiosiroid diatoms. *Front. Microbiol.* 2:234.

Zielinski, U. & Gersonde, R. 1997. Diatom distributions in Southern Ocean surface sediments (Atlantic sector): implications for paleoenvironmental reconstructions. *Palaeogeogr. Palaeoclimatol. Palaeoecol.* 129:213–50.

## Supporting Information

Additional Supporting Information may be found in the online version of this article at the publisher's web site:

**Figure S1.** Growth characteristics of *Pseudo-nitzschia granii* used for the comparative transcriptomic analysis. Plotted are the natural log of relative fluorescence units (RFU; black circles) and the maximum photochemical yield of PSII ($F_v$:$F_m$; gray circles) as a function of time before and after iron resupply to iron-limited cells (indicated by arrow).

**Figure S2.** Dissolved $NO_3$ concentrations (gray bars) and total chlorophyll *a* concentrations (colored bars) in iron grow-out experiments of natural phytoplankton communities performed at Ocean Station Papa, Gulf of Alaska in (a) 2013 and (b) 2015, and the California upwelling zone (c–e) in 2014 (see Fig. 4 for experiment locations). For each experiment, concentrations are provided for an iron-amended treatment (Fe), unamended control treatment (Ctrl), and desferroxamine B treatment (DFB; except for a). Numbers denote incubation times in hours. Where provided, error bars are the standard deviation of the mean of triplicate incubations.

**Table S1.** Total iron concentrations ($Fe_T$) and the predicted dissolved inorganic iron concentrations ($Fe'$) for the iron treatments used in this study. The conditional stability constants used to predict $Fe'$ were obtained from Sunda et al. 2005, which assumes a 100 $\mu mol \cdot L^{-1}$ EDTA metal ion buffer system in seawater at 20°C, a pH of 8.2, and a salinity of 36. For our culture experiments, actual conditional stability constants may slightly differ due to variations in growth temperature and salinity.

**Table S2.** Gene information and primer sequences.

**Table S3.** Expression of select genes in the *Pseudo-nitzschia granii* comparative transcriptome. Listed are the log (base 2) fold-change ratio of the normalized transcript abundance of the iron-resupplied cells over the iron-limited cells (R) and the average of the read counts in the iron-resupplied and iron-limited sequence libraries for each gene (A). Where available, KEGG Ortholog (KO) IDs are also provided. N/A = not available.